Theory of charge transport in diffusive normal metal/conventional superconductor point contacts

Y. Tanaka,[1] A. A. Golubov,[2] and S. Kashiwaya[3]

[1]*Department of Applied Physics, Nagoya University, Nagoya 464-8603, Japan*
[2]*Faculty of Science and Technology, University of Twente, 7500 AE, Enschede, The Netherlands*
[3]*National Institute of Advanced Industrial Science and Technology, Tsukuba 305-8568, Japan*

Tunneling conductance in diffusive normal (DN) metal/insulator/s-wave superconductor junctions is calculated for various situations by changing the magnitudes of the resistance and Thouless energy in DN and the transparency of the insulating barrier. The generalized boundary condition introduced by Nazarov [Superlattices and Microstructures **25**, 1221 (1999)] is applied, where the ballistic theory by Blonder, Tinkham, and Klapwijk and the diffusive theory by Volkov, Zaitsev, and Klapwijk based on the boundary condition of Kupriyanov and Lukichev are naturally reproduced. It is shown that the proximity effect can enhance (reduce) the tunneling conductance for junctions with a low (high) transparency. A wide variety of dependencies of tunneling conductance on voltage bias is demonstrated including a U-shaped gap like structure, a zero-bias conductance peak, and a zero-bias conductance dip. The temperature dependence of tunneling conductance is also calculated, and the conditions for the reentrance effect are studied.

I. INTRODUCTION

The electron coherence in mesoscopic superconducting systems is one of the important topics of solid-state physics. The low-energy transport in these systems is essentially influenced by the Andreev reflection,[1] a unique process specific for normal metal/superconductor interfaces. The phase coherence between incoming electrons and Andreev reflected holes persists in the diffusive normal metal at a mesoscopic length scale and results in strong interference effects on the probability of Andreev reflection.[2] These effects become prominent at sufficiently low temperatures where the thermal broadening is negligible. One of the remarkable experimental manifestations is the zero-bias conductance peak (ZBCP).[3–13] A calculation of tunneling conductance in a normal metal (N)/superconductor (S) junction is an interesting theoretical problem since quantum interference effects due to Andreev reflection are expected.

For a clean NS contact in the presence of the interface potential barrier, the conductance was calculated by Blonder, Tinkham, and Klapwijk[14] (BTK) in terms of the corresponding transmission coefficients on the basis of the solution of the Bogoliubov–de Gennes equations. From the general set of boundary conditions connecting the quasiclassical Green's functions on both sides of the interface for arbitrary transmission probabilities, Zaitsev[15] derived the expression for the conductance similar to that by BTK. The BTK method[14] is confined to ballistic systems. The generalization of this method to systems with impurities has been performed by several authors (see the review in Ref. 16). In a number of papers, the transmission coefficients were directly calculated by numerical methods.[17,18] However, it is difficult to apply such methods to most of relevant experimental situations. Another approach, the so-called random matrix theory, was employed by Beenakker *et al.*, where the total transmission coefficients are expressed in terms of those through the normal part of the system and the normal/superconductor interface separately.[16,19] Within this theory, the ZBCP observed in

experiments is understood as a resonance phenomenon related to reflectionless tunneling.[20] The scattering matrix approach was later generalized to finite voltage and temperature.[21]

On the other hand, a quasiclassical Green's function calculation based on nonequilibrium superconductivity theories[22] is much more powerful and convenient for the actual calculations.[23] In this approach, the impurity scattering is included in the self-consistent Born approximation and the weak localization effects are neglected. In the theory of tunneling conductance developed by Volkov, Zaitsev, and Klapwijk (VZK) by solving the Usadel equations,[24] the origin of the ZBCP observed in several experiments was clarified to be due to the enhancement of the pair amplitude in the diffusive normal metal by the proximity effect.[23] VZK applied the Kupriyanov and Lukichev (KL) boundary condition for the Keldysh-Nambu Green's function.[25] The KL boundary condition is valid for the atomically sharp interface barrier dividing two diffusive metals. As shown by Lambert *et al.*,[26] this condition is exact in two limits of either high or low barrier transparency, with small corrections in the intermediate transparency range. By applying the VZK theory, several authors studied the charge transport in various junctions[27–34] by solving the Usadel equations (see the review by Belzig *et al.*[35])

The generalization of the KL boundary conditions for an arbitrary connector between diffusive metals was provided by Nazarov within the so-called "generalized circuit theory."[36] In this theory, the mesoscopic system is presented as a network of nodes and connectors. A connector is characterized by a set of transmission coefficients and can present anything from a ballistic point contact to a tunnel junction. A conservation law of matrix current holds in each node. The method to derive the relation between matrix current and Green's functions puts the results of Ref. 15 to the framework of Landauer-Büttiker scattering formalism. The boundary condition for Keldysh-Nambu Green's function was derived in Ref. 36 for an arbitrary connector including

various situations from ballistic point contact to diffusive contact. Actually, this boundary condition is very general since the BTK theory is reproduced in the ballistic limit while in the diffusive limit with a low transmissivity of the interface, the KL boundary condition is reproduced.

Although a number of papers were published on charge transport in mesoscopic NS junctions, as far as we know, almost all of them are either based on the KL boundary conditions or on the BTK model. However, in the actual junctions, transparency of the junction is not necessarily small and impurity scattering in the DN is important. Therefore, an interesting and important theoretical problem is the calculation of the tunneling conductance in normal metal/conventional superconductor junctions using the boundary condition from Ref. 36 since both the ballistic (BTK theory) and diffusive (VZK theory) cases can be covered simultaneously. In the present paper, we study the tunneling conductance in diffusive normal metal/insulator/conventional superconductor (DN/I/S) junctions for various parameters such as the height of the insulating barrier at the interface, resistance R_d in DN, and the Thouless energy E_{Th} in DN. We concentrate on the normalized tunneling conductance of the junctions $\sigma_T(eV)$ as a function of the bias voltage V. The conductance $\sigma_T(eV)$ is given by $\sigma_T(eV) = \sigma_S(eV)/\sigma_N(eV)$, where $\sigma_{S(N)}(eV)$ is the tunneling conductance in the superconducting (normal) state at a bias voltage V.

In the present paper, the following points are clarified:

(1) When the transparency of the junction is sufficiently low, $\sigma_T(eV)$ for $|eV| < \Delta_0$ is enhanced with the increase of R_d due to the enhancement of the proximity effect. The ZBCP becomes prominent for $E_{Th} \ll \Delta_0$ and $R_d/R_b < 1$. In such a case, with a further increase of R_d/R_b, the ZBCP changes into a zero bias conductance dip (ZBCD). In the low transparent limit, the line shapes of $\sigma_T(eV)$ are qualitatively the same as those obtained by the VZK theory.[23,28]

(2) When the transparency of the junction is almost unity, $\sigma_T(eV)$ always exhibits a ZBCD except for the special case of $R_d = 0$, i.e., the BTK limit.

(3) The measure of the proximity effect, θ, is mainly determined by R_d/R_b and E_{Th}, where R_b is the resistance from the insulating barrier. The proximity effect enhances (reduces) the magnitude of $\sigma_T(eV)$ for junctions with low (high) transparency.

(4) Even for junctions between conventional s-wave superconductors, we can expect a wide variety of line shapes of the tunneling conductance, a ZBCP, ZBCD, U-shaped structure, and a rounded bottom structure.

(5) We have clarified the parameter space where a ZBCP should be expected. Typically, small Thouless energy E_{Th} is required for a ZBCP. If the magnitude of E_{Th} is increasing up to Δ_0, a ZBCP is only expected for junctions with low transmissivity, $R_d/R_b \ll 1$.

The organization of this paper is as follows. In Sec. II, we will provide the detailed derivation of the expression for the normalized tunneling conductance. In Sec. III, the results of calculations of $\sigma_T(eV)$ and θ are presented for various types of junctions. In Sec. IV, the summary of the obtained results is given.

II. FORMULATION

In this section we introduce the model and the formalism. We consider a junction consisting of normal and superconducting reservoirs connected by a quasi-one-dimensional diffusive conductor (DN) with a length L much larger than the mean free path. The interface between the DN conductor and the S electrode has a resistance R_b, while the DN/N interface has zero resistance. The positions of the DN/N interface of the DN/S interface are denoted as $x = 0$ and $x = L$, respectively. According to the circuit theory, the interface between DN and S is subdivided into two isotropization zones in DN and S, two ballistic zones, and a scattering zone. The sizes of the ballistic and scattering zones in the current flow direction are much shorter than the coherence length. Although the generalized boundary condition of Ref. 36 is valid for arbitrary interfaces, here scattering zone is modeled as an infinitely narrow insulating barrier described by the delta function $U(x) = H\delta(x-L)$. The resulting transparency of the junctions T_m is given by $T_m = 4\cos^2\phi/(4\cos^2\phi + Z^2)$, where $Z = 2H/(\hbar v_F)$ is a dimensionless constant, ϕ is the injection angle measured from the interface normal to the junction and v_F is Fermi velocity. Variation of the barrier shape will not change our results in the considered case of isotropic superconductivity in the S electrode.

We apply the quasiclassical Keldysh formalism in the following calculation of the tunneling conductance. The 4×4 Green's functions in DN and S are denoted by $\check{G}_1(x)$ and $\check{G}_2(x)$, which are expressed in matrix form as

$$\check{G}_1(x) = \begin{pmatrix} \hat{R}_1(x) & \hat{K}_1(x) \\ 0 & \hat{A}_1(x) \end{pmatrix}, \tag{1}$$

$$\check{G}_2(x) = \begin{pmatrix} \hat{R}_2(x) & \hat{K}_2(x) \\ 0 & \hat{A}_2(x) \end{pmatrix}, \tag{2}$$

where the Keldysh component $\hat{K}_{1,2}(x)$ is given by $\hat{K}_{1(2)}(x) = \hat{R}_{1(2)}(x)\hat{f}_{1(2)}(x) - \hat{f}_{1(2)}(x)\hat{A}_{1(2)}(x)$, with retarded component $\hat{R}_{1,2}(x)$, advanced component $\hat{A}_{1,2}(x)$, using distribution function $\hat{f}_{1(2)}(x)$. In the above, $\hat{R}_2(x)$ is expressed by

$$\hat{R}_2(x) = (g\hat{\tau}_3 + f\hat{\tau}_2),$$

with $g = \epsilon/\sqrt{\epsilon^2 - \Delta_0^2}$ and $f = \Delta_0/\sqrt{\Delta_0^2 - \epsilon^2}$, where ϵ denotes the quasiparticle energy measured from the Fermi energy, $\hat{A}_2(x) = -\hat{R}_2^*(x)$, and $\hat{f}_2(x) = \tanh[\epsilon/(2k_BT)]$ in thermal equilibrium with temperature T. We put the electrical potential zero in the S electrode. In this case the spatial dependence of $\check{G}_1(x)$ in DN is determined by the static Usadel equation,[24]

$$D\frac{\partial}{\partial x}\left[\check{G}_1(x)\frac{\partial \check{G}_1(x)}{\partial x}\right] + i[\check{H}, \check{G}_1(x)] = 0, \tag{3}$$

with the diffusion constant D in DN, where $\check{H}$ is given by

$$\check{H}=\begin{pmatrix} \hat{H}_0 & 0 \\ 0 & \hat{H}_0 \end{pmatrix},$$

with $\hat{H}_0 = \epsilon \tau_3$.

The boundary condition for $\check{G}_1(x)$ at the DN/S interface is given by Nazarov's generalized boundary condition,

$$\frac{L}{R_d}\left(\check{G}_1 \frac{\partial \check{G}_1}{\partial x}\right)\Bigg|_{x=L_-} = R_b^{-1}\langle B\rangle, \tag{4}$$

$$B = \frac{2T_m[\check{G}_1(L_-),\check{G}_2(L_+)]}{4+T_m([\check{G}_1(L_-),\check{G}_2(L_+)]_+ - 2)}.$$

The average over the various angles of injected particles at the interface is defined as

$$\langle B(\phi)\rangle = \int_{-\pi/2}^{\pi/2} d\phi \cos\phi B(\phi) \Bigg/ \int_{-\pi/2}^{\pi/2} d\phi T(\phi)\cos\phi,$$

with $B(\phi)=B$ and $T(\phi)=T_m$. The resistance of the interface (R_b) is given by

$$R_b = R_0 \frac{2}{\displaystyle\int_{-\pi/2}^{\pi/2} d\phi T(\phi)\cos\phi}.$$

Here R_0 is the Sharvin resistance, which in three-dimensional case is given by $R_0^{-1} = e^2 k_F^2 S_c/(4\pi^2\hbar)$, where k_F is the Fermi wave vector and S_c is the constriction area. Note that the area S_c is in general not equal to the cross-section area S_d of the normal conductor; therefore S_c/S_d is an independent parameter of our theory.

For $T_m \to 0$ in Eq. (4), the quantity B can be expressed as

$$B = \frac{T_m}{2}[\check{G}_1,\check{G}_2],$$

and we can reproduce the KL boundary condition. On the other hand, at $x=0$, $\check{G}_1(0)$ coincides with that in the normal state.

The electric current is expressed using $\check{G}_1(x)$ as

$$I_{el} = \frac{-L}{4eR_d}\int_0^\infty d\epsilon \mathrm{Tr}\left[\tau_3\left(\check{G}_1(x)\frac{\partial\check{G}_1(x)}{\partial x}\right)^K\right], \tag{5}$$

where $(\check{G}_1(x)[\partial\check{G}_1(x)/\partial x])^K$ denotes the Keldysh component of $(\check{G}_1(x)[\partial\check{G}_1(x)/\partial x])$. In the actual calculation it is convenient to use the standard θ parametrization when function $\hat{R}_1(x)$ is expressed as

$$\hat{R}_1(x) = \hat{\tau}_3 \cos\theta(x) + \hat{\tau}_2 \sin\theta(x). \tag{6}$$

The parameter $\theta(x)$ is a measure of the proximity effect in DN.

Functions $\hat{A}_1(x)$ and $\hat{K}_1(x)$ are expressed as $\hat{A}_1(x) = -\hat{R}_1^*(x)$ and $\hat{K}_1(x) = \hat{R}_1(x)\hat{f}_1(x) - \hat{f}_1(x)\hat{A}_1(x)$, with the distribution function $\hat{f}_1(x)$ given by $\hat{f}_1(x) = f_l(x) + \hat{\tau}_3 f_t(x)$.

In the above, $f_t(x)$ is the relevant distribution function which determines the conductance of the junction we are now concentrating on. From the retarded or advanced component of the Usadel equation, the spatial dependence of $\theta(x)$ is determined by the following equation

$$D\frac{\partial^2}{\partial x^2}\theta(x) + 2i\epsilon \sin[\theta(x)] = 0, \tag{7}$$

while for the Keldysh component we obtain

$$D\frac{\partial}{\partial x}\left[\frac{\partial f_t(x)}{\partial x}\cosh^2\theta_{im}(x)\right] = 0. \tag{8}$$

At $x=0$, since DN is attached to the normal electrode, $\theta(0)=0$, and $f_t(0)=f_{t0}$ is satisfied with

$$f_{t0} = \frac{1}{2}\{\tanh[(\epsilon+eV)/(2k_BT)] - \tanh[(\epsilon-eV)/(2k_BT)]\}.$$

Next we focus on the boundary condition at the DN/S interface. Taking the retarded part of Eq. (4), we obtain

$$\frac{L}{R_d}\frac{\partial\theta(x)}{\partial x}\Bigg|_{x=L_-} = \frac{\langle F\rangle}{R_b}, \tag{9}$$

$$F = \frac{2(f\cos\theta_L - g\sin\theta_L)T_m}{(2-T_m)+T_m[g\cos\theta_L + f\sin\theta_L]},$$

with $\theta_L = \theta(L_-)$.

On the other hand, from the Keldysh part of Eq. (4), we obtain

$$\frac{L}{R_d}\left(\frac{\partial f_t}{\partial x}\right)\cosh^2\theta_{im}(x)\Bigg|_{x=L_-} = -\frac{\langle I_{b0}\rangle f_t(L_-)}{R_b}, \tag{10}$$

with

$$I_{b0} = \frac{T_m^2\Lambda_1 + 2T_m(2-T_m)\Lambda_2}{2|(2-T_m)+T_m[g\cos\theta_L + f\sin\theta_L]|^2},$$

$$\Lambda_1 = (1+|\cos\theta_L|^2+|\sin\theta_L|^2)(|g|^2+|f|^2+1)$$
$$+4\mathrm{Im}[fg^*]\mathrm{Im}[\cos\theta_L\sin\theta_L^*], \tag{11}$$

$$\Lambda_2 = \mathrm{Re}\{g(\cos\theta_L + \cos\theta_L^*) + f(\sin\theta_L + \sin\theta_L^*)\}, \tag{12}$$

where $\theta_{im}(x)$ denotes the imaginary part of $\theta(x)$. For $T_m \ll 1$, I_{b0} is reduced to

$$I_{b0} = \frac{\mathrm{Re}[g(\cos\theta_L + \cos\theta_L^*) + f(\sin\theta_L + \sin\theta_L^*)]}{2}T_m, \tag{13}$$

which is the expression used in the VZK theory. After a simple manipulation, we can obtain $f_t(L_-)$

$$f_t(L_-) = \frac{R_b f_{t0}}{R_b + \frac{R_d\langle I_{b0}\rangle}{L}\displaystyle\int_0^L \frac{dx}{\cosh^2\theta_{im}(x)}}.$$
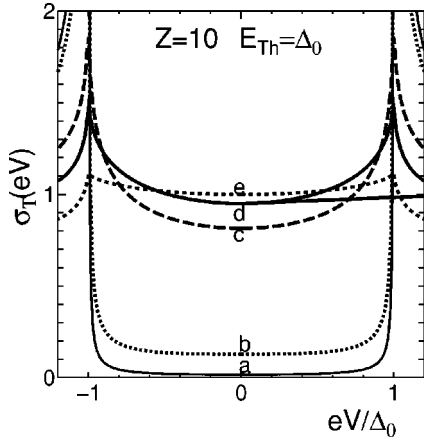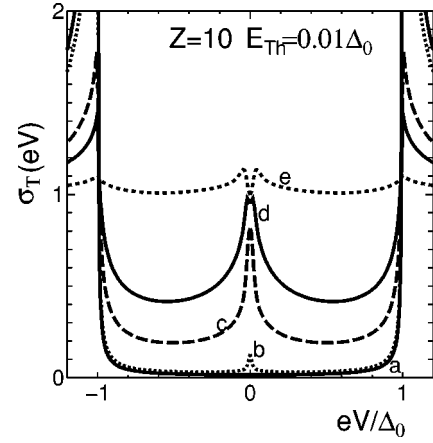
FIG. 1. Normalized tunneling conductance for $Z=10$ and $E_{Th}/\Delta_0=1$. (a) $R_d/R_b=0$, (b) $R_d/R_b=0.1$, (c) $R_d/R_b=1$, (d) $R_d/R_b=2$, and (e) $R_d/R_b=10$.

Since the electric current I_{el} can be expressed via θ_L in the following form,

$$I_{el}=-\frac{L}{eR_d}\int_0^\infty \left(\frac{\partial f_t}{\partial x}\right)\bigg|_{x=L_-} \cosh^2[\mathrm{Im}(\theta_L)]d\epsilon,$$

we obtain the following final result for the current:

$$I_{el}=\frac{1}{e}\int_0^\infty d\epsilon \frac{f_{t0}}{\dfrac{R_b}{\langle I_{b0}\rangle}+\dfrac{R_d}{L}\displaystyle\int_0^L \frac{dx}{\cosh^2\theta_{im}(x)}}. \quad (14)$$

Then the total resistance R at zero temperature is given by

$$R=\frac{R_b}{\langle I_{b0}\rangle}+\frac{R_d}{L}\int_0^L \frac{dx}{\cosh^2\theta_{im}(x)}, \quad (15)$$

and the tunneling conductance in the superconducting state $\sigma_S(eV)$ is given by $\sigma_S(eV)=1/R$.

It should be mentioned that for $R_d=0$, θ_L becomes zero due to the absence of the proximity effect. Then I_{b0} is given as follows:

$$I_{b0}=\frac{(1+|g|^2+|f|^2)T_m^2+2T_m(2-T_m)\mathrm{Re}(g)}{|(2-T_m)+T_mg|^2}$$

$$=\frac{T_m[1+|\Gamma|^2+(T_m-1)|\Gamma|^4]}{|1-(1-T_m)\Gamma^2|^2}, \quad (16)$$

with $\Gamma=(\epsilon-\sqrt{\epsilon^2-\Delta_0^2})^{1/2}/(\epsilon+\sqrt{\epsilon^2-\Delta_0^2})^{1/2}$ and the resulting σ_S is given by

$$\sigma_S(eV)=\frac{1}{R_0}\int_{-\pi/2}^{\pi/2}\frac{I_{b0}}{2}\cos\phi d\phi,$$

and reproduces that by BTK theory.

It should be remarked that in the present circuit theory, R_d/R_b can be varied independently of T_m, i.e., independently of Z, since one can change the magnitude of the constriction area S_c independently. In other words, R_d/R_b is no

more proportional to $T_{av}(L/l)$, where T_{av} is the averaged transmissivity of the barrier and l is the mean free path in the diffusive region, respectively. Based on this fact, we can choose R_d/R_b and Z as independent parameters.

In the following section, we will discuss the normalized tunneling conductance $\sigma_T(eV)=\sigma_S(eV)/\sigma_N(eV)$, where $\sigma_N(eV)$ is the tunneling conductance in the normal state given by $\sigma_N(eV)=\sigma_N=1/(R_d+R_b)$, respectively.

III. RESULTS

A. Tunneling conductance vs voltage: Zero-bias anomalies

In this section, we focus on the line shape of the tunneling conductance. Let us first choose the relatively strong barrier $Z=10$ (Figs. 1 and 2) for various R_d/R_b. For $E_{Th}=\Delta_0$, the magnitude of $\sigma_T(eV)$ for $|eV|<\Delta_0$ increases with the increase of R_d/R_b. First, the line shape of the tunneling conductance remains to be U shaped and only the height of the bottom value is enhanced (curve b). Then, with a further increase of R_d/R_b, a rounded bottom structure (curves c and d) appears, and finally it changes into a nearly flat line shape (curve e). For $E_{Th}=0.01\Delta_0$ (Fig. 2), the magnitude of

FIG. 2. Normalized tunneling conductance for $Z=10$ and $E_{Th}/\Delta_0=0.01$. (a) $R_d/R_b=0$, (b) $R_d/R_b=0.1$, (c) $R_d/R_b=1$, (d) $R_d/R_b=2$, (e) $R_d/R_b=10$.
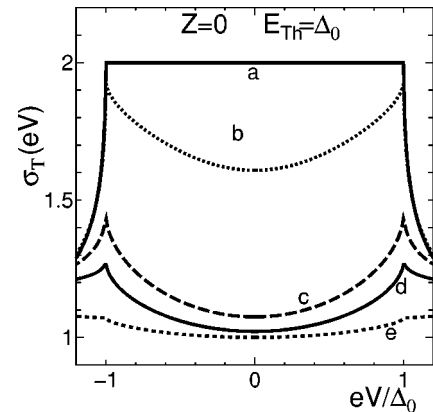

FIG. 3. Normalized tunneling conductance for $Z=0$ and $E_{Th}/\Delta_0=1$. (a) $R_d/R_b=0$, (b) $R_d/R_b=0.1$, (c) $R_d/R_b=1$, (d) $R_d/R_b=2$, and (e) $R_d/R_b=10$.
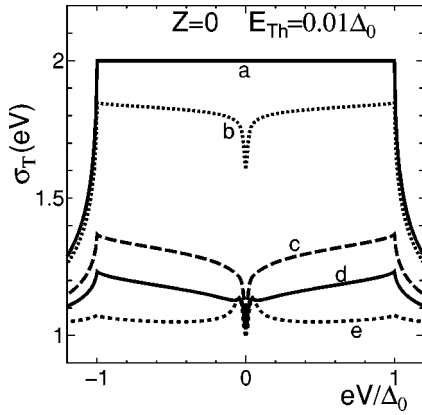
FIG. 4. Normalized tunneling conductance for $Z=0$ and $E_{Th}/\Delta_0=0.01$. (a) $R_d/R_b=0$, (b) $R_d/R_b=0.1$, (c) $R_d/R_b=1$, (d) $R_d/R_b=2$, and (e) $R_d/R_b=10$.

$\sigma_T(eV)$ has a ZBCP once the magnitude of R_d/R_b deviates slightly from 0. The order of magnitude of the ZBCP width is given by E_{Th}. When the magnitude of R_d/R_b, exceeds unity, the ZBCP splits into two (curve d), and finally $\sigma_T(eV)$ acquires a ZBCD (curve e). In the limit of an extremely strong barrier with $Z\to\infty$, the results of the VZK theory are reproduced.

On the other hand, in the fully transparent case with $Z=0$, the line shape of the tunneling conductance becomes quite different. For $E_{Th}=\Delta_0$ (Fig. 3), the magnitude of $\sigma_T(eV)$ decreases with the increase of the magnitude of R_d/R_b. The bottom parts of all curves are rounded and $\sigma_T(eV)$ always exceeds unity. On the other hand, for $E_{Th}=0.01\Delta_0$, $\sigma_T(eV)$ has a ZBCD even for a small magnitude of R_d/R_b except for the special case of $R_d/R_b=0$ where the BTK theory is valid (see Fig. 4). This feature is quite different from that shown in Fig. 2. In the case of an intermediate barrier strength, $Z=1$, the shape of $\sigma_T(eV)$ becomes rather complex (Figs. 5 and 6). For $E_{Th}=\Delta_0$, $\sigma_T(eV)$ has a shallow gap structure similar to the case of the BTK theory (curve a). With the increase of R_d/R_b, the coherent peak structure at $eV=\pm\Delta_0$ is smeared out and the voltage depen-
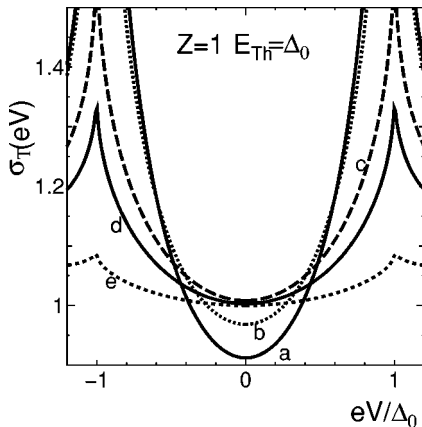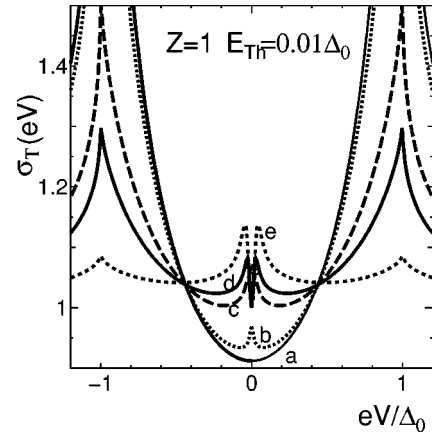

FIG. 6. Normalized tunneling conductance for $Z=1$ and $E_{Th}/\Delta_0=0.01$. (a) $R_d/R_b=0$, (b) $R_d/R_b=0.1$, (c) $R_d/R_b=1$, (d) $R_d/R_b=2$, and (e) $R_d/R_b=10$.

dence becomes very weak as shown by curve e. For $E_{Th}=0.01\Delta_0$, the ZBCP appears for a small magnitude of R_d/R_b (see curve b). With increasing magnitude of R_d/R_b, the ZBCP changes into a ZBCD (curves $c-e$). As compared to the $Z=10$ case (see Fig. 2), the ZBCP is much more easier to change into a ZBCD by increasing the magnitude of R_d/R_b.

It is interesting to study how various parameters influence the proximity effect. The measure of the proximity effect at the S/N interface θ_L is plotted for $Z=0$ and 10 with corresponding parameters in Figs. 1–4. For $R_d/R_b=0$, $\theta_L=0$ is satisfied for any E_{Th} and Z. Besides this fact, at $\epsilon=0$, θ_L always becomes a real number. First, we study value of the case of $E_{Th}/\Delta_0=1$ (Fig. 7) where the same values of R_d/R_b are chosen as in Figs. 1 and 3. The real part of θ_L is enhanced with an increase in R_d/R_b and is almost constant as a function of ϵ. At the same time, the imaginary part of θ_L is an increasing function of ϵ for all cases. There is no clear qualitative difference between the energy dependencies of Re(θ_L) and Im(θ_L) at $Z=0$ and 10. Next, we discuss the line shapes of θ_L for $E_{Th}/\Delta_0=0.01$ (Fig. 8). Re(θ_L) has a
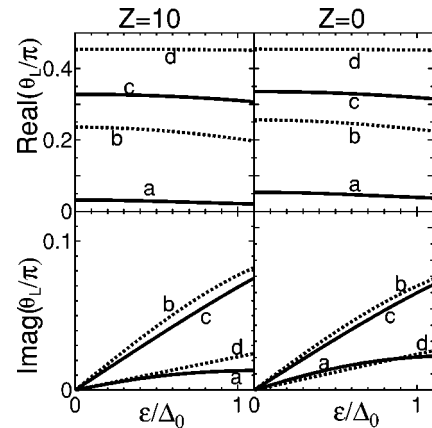

FIG. 5. Normalized tunneling conductance for $Z=1$ and $E_{Th}/\Delta_0=1$. (a) $R_d/R_b=0$, (b) $R_d/R_b=0.1$, (c) $R_d/R_b=1$, (d): $R_d/R_b=2$, and (e) $R_d/R_b=10$.

FIG. 7. Real (upper panels) and imaginary parts of θ_L (lower panels) are plotted as a function of ϵ. $Z=10$ (left panels) and $Z=0$ (right panels), with $E_{Th}/\Delta_0=1$. (a) $R_d/R_b=0.1$, (b) $R_d/R_b=1$, (c) $R_d/R_b=2$, (d) $R_d/R_b=10$.

peak at zero voltage and decreases with the increase of ϵ. $\text{Im}(\theta_L)$ increases sharply from 0 and has a peak at about $\epsilon \sim E_{Th}$, except for a sufficiently large value of R_d. Also in this case, there is no qualitative difference between the line shapes of $\text{Re}(\text{Im})(\theta_L)$ for the $Z=0$ case and that for $Z=10$.

Although the magnitude of θ_L, i.e., the measure of proximity effect, is enhanced with increasing R_d/R_b, its influence on $\sigma_T(eV)$ is different for low and high transparent junctions. In the low transparent junctions, the increase in the magnitude of θ_L by R_d/R_b can enhance the conductance $\sigma_T(eV)$ for $eV \sim 0$ and produce a ZBCP, whereas in high transparent junctions the enhancement of θ_L suppresses the magnitude of $\sigma_T(eV)$.

Finally, we focus on the condition where the ZBCP appears. We change Z and R_d/R_b for fixed E_{Th}. An upper critical value of $R_d = R_{bu}$ exists, where the ZBCP vanishes for $R_d > R_{bu}$. For $E_{Th} = 0.01\Delta_0$, R_{bu} increases with Z and converges at nearly 1.4. For $E_{Th} = 0.8\Delta_0$, the lower critical value of $R_d = R_{bl}$ also appears where the ZBCP vanishes for $R_d < R_{bl}$. The ZBCP is expected for $R_{bl} < R_d < R_{bu}$. The magnitude of R_{bu} is suppressed drastically as compared to that for $E_{Th} = 0.01\Delta_0$. For $E_{Th} > \Delta_0$, a ZBCP region vanishes for $0 < Z < 20$. In order to understand the crossover from the ZBCP to the ZBCD in much more detail, it is interesting to calculate the second derivative of the total resistance R as a function of $\epsilon = eV$ at $\epsilon = 0$. For simplicity, here we focus on the case of a sufficiently large Z. For $\epsilon < \Delta_0$, for simplicity, the total resistance is written as

$$R = R_1 + R_2, \tag{17}$$

$$R_1 = \frac{R_b}{\langle I_{b0} \rangle}, \quad R_2 = \frac{R_d}{L} \int_0^L \frac{dx}{\cosh^2 \theta_i(x)},$$

$$\langle I_{b0} \rangle = f \sin \theta_{L,r} \cosh \theta_{L,i},$$

with $\theta_L = \theta_{L,r} + i\theta_{L,i}$, where $\theta_{L,r}$ and $\theta_{L,i}$ are the real and imaginary parts of θ_L, respectively. The second derivative of I_{b0} at $\epsilon = 0$ is given by

$$\frac{\partial^2 I_{b0}}{\partial \epsilon^2} = \frac{\sin \theta_{L,r}}{\Delta_0^2} + \cos \theta_{L,r} \frac{\partial^2 \theta_{L,r}}{\partial \epsilon^2} + \sin \theta_{L,r} \left(\frac{\partial \theta_{L,i}}{\partial \epsilon} \right)^2,$$

since $\partial \theta_{L,r}/\partial \epsilon = 0$ and $\theta_{L,i} = 0$ is satisfied at $\epsilon = 0$.

The resulting second derivative of the total resistance at zero energy is given as

$$\frac{\partial^2 R}{\partial \epsilon^2} = \frac{\partial^2 R_1}{\partial \epsilon^2} + \frac{\partial^2 R_2}{\partial \epsilon^2},$$

$$\frac{\partial^2 R_1}{\partial \epsilon^2} = -\frac{R_b}{\sin^2 \theta_{L,r}} \left[\frac{\sin \theta_{L,r}}{\Delta_0^2} + \cos \theta_{L,r} \frac{\partial^2 \theta_{L,r}}{\partial \epsilon^2} \right.$$

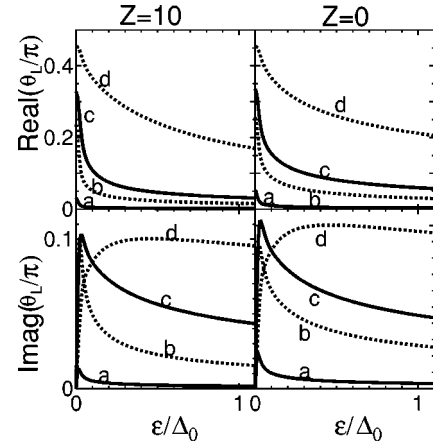$$\left. + \sin \theta_{L,r} \left(\frac{\partial \theta_{L,i}}{\partial \epsilon} \right)^2 \right], \tag{18}$$

FIG. 8. Real (upper panels) and imaginary parts of θ_L (lower panels) are plotted as a function of ϵ. $Z = 10$ (left panels) and $Z = 0$ (right panels), with $E_{Th}/\Delta_0 = 0.01$. (a) $R_d/R_b = 0.1$, (b) $R_d/R_b = 1$, (c) $R_d/R_b = 2$, and (d) $R_d/R_b = 10$.

$$\frac{\partial^2 R_2}{\partial \epsilon^2} = -\frac{2R_d}{L} \int_0^L \left[\frac{\partial \theta_i(x)}{\partial \epsilon} \right]^2 dx, \tag{19}$$

where $\theta_i(x)$ is the imaginary part of $\theta(x)$. The sign of $\partial^2 \theta_{L,r}/\partial \epsilon^2$ becomes negative and it can induce $\partial^2 R_1/\partial \epsilon^2 > 0$ in some cases. The order of $\partial^2 \theta_{L,r}/\partial \epsilon^2$ and $(\partial \theta_{L,i}/\partial \epsilon)^2$ is proportional to the inverse of E_{Th}^2. The sign of $\partial^2 R_1/\partial \epsilon^2$ is crucially influenced by the relative magnitude of the second term at the right-hand side of Eq. (18). On the other hand, the sign of $\partial^2 R_2/\partial \epsilon^2$ is always negative.

For $E_{Th} \ll \Delta_0$ and small magnitude of R_d/R_b, the resulting $\theta_{L,r}$ is sufficiently small and the magnitude of $\partial^2 R_1/\partial \epsilon^2$ becomes positive. When this positive contribution overcomes the negative contribution from $\partial^2 R_2/\partial \epsilon^2$, we can expect a resistance minimum at zero energy, i.e., a ZBCP. However, with increasing R_d/R_b, the magnitude of $\partial^2 R_1/\partial \epsilon^2$ decreases due to the enhancement of the third term in the right-hand side of Eq. (18), while $\partial^2 R_2/\partial \epsilon^2$ increases. Then, a critical value $R_d = R_{bu}$ appears, above which the ZBCP changes into a ZBCD with an increase of R_d/R_b. This is the mechanism of the crossover from a ZBCP to a ZBCD.

When the magnitude of E_{Th} is enhanced, the magnitudes of the second and third terms in Eq. (18) are reduced, and the first term can not be neglected. The resulting magnitude of
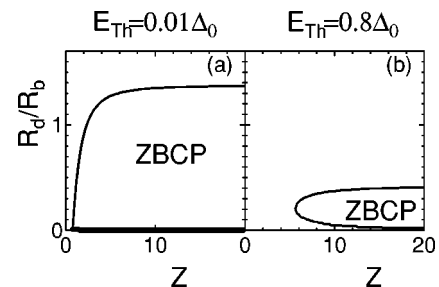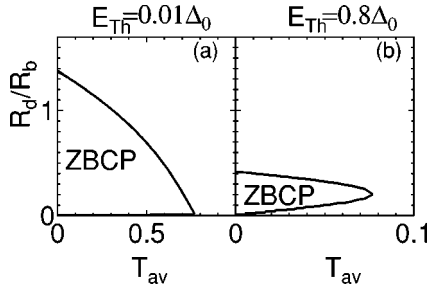

FIG. 9. The parameter space where ZBCP appears.

FIG. 10. Similar plots as in Fig. 9 using T_{av}.

$\partial^2 R_1 / \partial \epsilon^2$ is suppressed and the value of R_{bu} is reduced. This is the origin of the difference in R_{bu} in Figs. 9(a) and 9(b).

It is also interesting to present similar plots as Fig. 9 using an averaged transparency of the junction T_{av},

$$T_{av} = \frac{\int_{-\pi/2}^{\pi/2} \cos\phi T(\phi) d\phi}{2}. \tag{20}$$

The results are shown in Fig. 10. For $E_{Th}=0.01\Delta_0$, the magnitude of R_{bu} decreases monotonically with increasing T_{av}, and it vanishes about $T_{av} \sim 0.8$. For $E_{Th}=0.8\Delta_0$, the magnitude of R_{bl} increases for an increasing T_{av}, while that for R_{bu} decreases. The ZBCP region is restricted to small values of R_d/R_b.

In any way, the preferred condition for the formation of a ZBCP is the combination of the low transparency of the junction and the smallness of the E_{Th}/Δ_0 ratio. This situation is understood as follows. It is well known from the BTK theory that the magnitude of the zero-bias conductance is almost proportional to T_{av}^2 for $R_d=0$ for $T_{av} \ll 1$. With the increase in the magnitude of R_d, the measure of the proximity effect θ_L is enhanced for $|\epsilon| < E_{Th}$, and the zero-bias conductance is proportional to T_{av}. However, the magnitude of θ_L at finite energy in the range $E_{Th} < |\epsilon| < \Delta_0$ is drastically suppressed as shown in Fig. 8, due to the existence of the proximity induced minigap[37] in the normal diffusive part DN
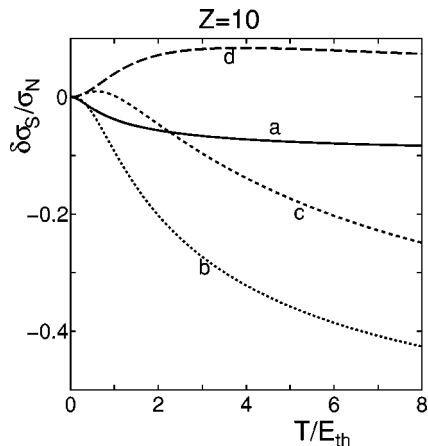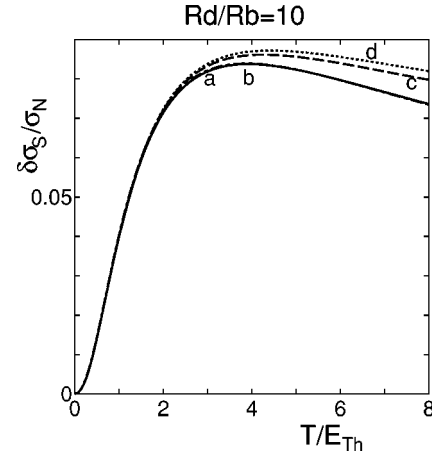

FIG. 12. $\delta\sigma_S/\sigma_N$ is plotted as a function of T. $R_d/R_b=10$ and $E_{Th}=0.01\Delta_0$. (a) VZK theory, (b) $Z=10$, (c) $Z=1$, and (d) $Z=0$.

of the order of E_{Th}. As a result, in this regime the conductance channel that provides a contribution proportional to T_{av} is not available. Thus only the low-voltage conductance is enhanced. On the other hand, for large E_{Th} with $E_{Th} \sim \Delta_0$, the measure of proximity effect θ_L is insensitive to energy for $|\epsilon| < \Delta_0$ (see Fig. 7), then the resulting $\sigma_T(eV)$ is always enhanced for $|eV| < \Delta_0$, and the degree of the prominent enhancement of $\sigma_T(0)$ is weakened.

B. Tunneling conductance vs temperature: Reentrance effect

Finally, we look at temperature dependence of conductance for various Z and R_d/R_b and focus on the relevance to the corresponding results in VZK theory based on the KL boundary condition. We calculate tunneling conductance at nonzero temperature following

$$\sigma_S(eV,T) = dI_{el}/dV. \tag{21}$$

Then we define deviation of tunneling conductance from that at zero temperature given by

$$\delta\sigma_S = \sigma_S(eV,T) - \sigma_S(eV,0). \tag{22}$$

In the following, we will plot $\delta\sigma_S/\sigma_N$ as a function of the temperature T (see Figs. 11–13).

For $R_d/R_b=0.1$ (curve a) and $R_d/R_b=1$ (curve b), due to the existence of ZBCP as shown in Fig. 2, $\delta\sigma_S/\sigma_N$ takes negative value and decreases with T. While for $R_d/R_b=2$, $\delta\sigma_S/\sigma_N$ first increases and decreases again (curve c). With the further increase of the magnitude of R_d/R_b, $\delta\sigma_S/\sigma_N$ becomes positive, and it has maximum at a certain temperature. This effect is known as "reentrance effect." It was predicted theoretically within the VZK theory in Ref. 29–31 and observed experimentally.[38] According to the theory,[29–31] for $R_b \to 0$, the maximum value of $\delta\sigma_S/\sigma_N$ is about 0.09 at temperature of the order of Thouless energy. Note that the reentrance of the metallic conductance occurs as a function of bias voltage as well, but here we concentrate on the temperature dependence since it was studied in most detail within the VZK theory.
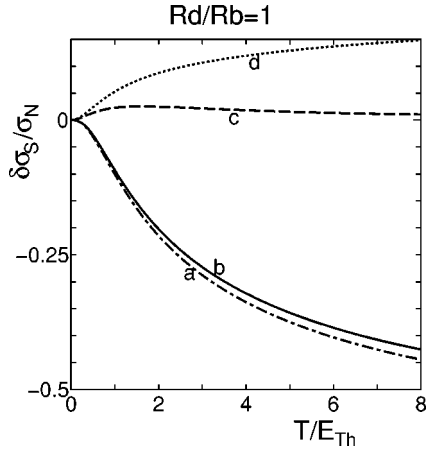

FIG. 11. $\delta\sigma_S/\sigma_N$ is plotted as a function of T. $Z=10$ and $E_{Th}=0.01\Delta_0$. (a) $R_d/R_b=0.1$, (b) $R_d/R_b=1$, (c) $R_d/R_b=2$, and (d) $R_d/R_b=10$.

FIG. 13. $\delta\sigma_S/\sigma_N$ is plotted as a function of T. $R_d/R_b=1$ and $E_{Th}=0.01\Delta_0$. (a) VZK theory, (b) $Z=10$, (c) $Z=1$, and (d) $Z=0$.

In order to study the consequences of our theory for the reentrance effect, we have calculated the temperature dependence of $\delta\sigma_S/\sigma_N$ for various Z for fixed R_d/R_b. For the comparison with the standard VZK theory, we also plot $\delta\sigma_S/\sigma_N$ using the KL boundary condition. For $R_d/R_b=10$, we always see the standard reentrant behavior. For $Z=10$, we cannot see clear deviation from the VZK theory (compare curves a and b). With the decrease of the magnitude of Z, the magnitude of $\delta\sigma_S/\sigma_N$ is enhanced much stronger (curves c and d). Although there are quantitative difference between four curves, the qualitative line shapes are similar to those predicted by the VZK theory.

However, situation is different for decreasing $R_d/R_b=1$. For $R_d/R_b=1$ the resulting $\delta\sigma_S/\sigma_N$ takes negative value and similar feature is also obtained for $Z=10$ (see curves a and b). At the same time, for small magnitude of Z, $\delta\sigma_S/\sigma_N$ takes positive value. As seen from these results, the deviation from VZK becomes significant for small magnitude of Z with $R_d/R_b<1$.

IV. CONCLUSIONS

In the present paper, a detailed theoretical investigation of the tunneling conductance of diffusive normal metal/conventional superconductor junctions is presented. Even for conventional s-wave junctions, the interplay between diffusive and interface scattering produces a wide variety of line shapes of the tunneling conductance: ZBCP, ZBCD, U-shaped, and rounded bottom structures. There are several points which have been clarified in this paper.

(1) When the transparency of a junction is sufficiently low and E_{Th} is small, the ZBCP appears for $R_d<R_b$. With an increase in R_d, the ZBCP changes into ZBCD. For large E_{Th} with the same order of Δ_0, the ZBCP is only expected for small values of R_d. With increasing E_{Th}, the ZBCP vanishes when $E_{Th}>\Delta_0$ is satisfied. For the low transparency limit, the results obtained by us are reduced to those by the VZK theory where the KL boundary condition is used.

(2) When the transparency of the junction is almost unity,

$\sigma_T(eV)$ always has a ZBCD except for the case of vanishing R_d.

(3) The proximity effect can enhance (reduce) the tunneling conductance of junctions with low (high) transparency.

The above-mentioned criteria for the existence of a ZBCP agree with available experimental data. However, we are not aware of an experimental observation of ZBCD in highly transparent junctions.

In the present paper, the superconductor is restricted to be a conventional s-wave superconductor. However, it is well known that a ZBCP also appears in unconventional superconductor junctions,[40,41] the origin of which is the formation of midgap Andreev bound states (MABS).[39] Indeed, a ZBCP has been reported in various superconductors that have an anisotropic pairing symmetry.[41,42] It should be remarked that the line shape of the ZBCP obtained in the present paper is quite different from that by MABS. In the present case, the height of $\sigma_T(eV)$ never exceeds unity, and its width is determined by E_{Th}; while in the MABS case, the peak height is proportional to the inverse of the magnitude of T_m, and the width is proportional to T_m.

The proper theory of transport of unconventional junctions in the presence of MABS has been formulated[40,41] only under the conditions of ballistic transport. Recently, this theory has been revisited to account for diffusive transport in the normal metal in Ref. 43, where an extension of the circuit theory was provided for unconventional superconductor junctions. A general relation was derived for matrix current B in Eq. (4), which is available for unconventional superconductor junctions with MABS. An elaborated example demonstrated the interplay of MABS and proximity effect in a d-wave junction. It is actually quite interesting to apply this circuit theory to the actual calculation of $\sigma_T(eV)$ as in the present paper. Such a direction of study is important in order to analyze recent tunneling experiments where mesoscopic interference effects were observed in high-T_C junction systems.[44] We will present the obtained results in the near future.[45]

In the present study, we have focused on N/S junctions. The extension of Nazarov's circuit theory to long diffusive S/N/S junctions has been performed by Bezuglyi et al.[33] In S/N/S junctions, the mechanism of multiple Andreev reflections produces the subharmonic gap structures on I-V curves[46–53] and the situation becomes much more complex as compared to N/S junctions. Moreover, in S/N/S junctions with unconventional superconductors, MABS lead to the anomalous current-phase relation and temperature dependence of the Josephson current.[54] An interesting problem is an extension of the circuit theory to S/N/S junctions with unconventional superconductors.

[1] A.F. Andreev, Sov. Phys. JETP **19**, 1228 (1996).

[2] F.W.J. Hekking and Yu.V. Nazarov, Phys. Rev. Lett. **71**, 1625 (1993).

[3] F. Giazotto, P. Pingue, F. Beltram, M. Lazzarino, D. Orani, S. Rubini, and A. Franciosi, Phys. Rev. Lett. **87**, 216808 (2001).

[4] T.M. Klapwijk, Physica B **197**, 481 (1994).

[5] A. Kastalsky, A.W. Kleinsasser, L.H. Greene, R. Bhat, F.P. Milliken, and J.P. Harbison, Phys. Rev. Lett. **67**, 3026 (1991).

[6] C. Nguyen, H. Kroemer, and E.L. Hu, Phys. Rev. Lett. **69**, 2847 (1992).

[7] B.J. van Wees, P. de Vries, P. Magnee, and T.M. Klapwijk, Phys. Rev. Lett. **69**, 510 (1992).

[8] J. Nitta, T. Akazaki, and H. Takayanagi, Phys. Rev. B **49**, 3659 (1994).

[9] S.J.M. Bakker, E. van der Drift, T.M. Klapwijk, H.M. Jaeger, and S. Radelaar, Phys. Rev. B **49**, 13 275 (1994).

[10] P. Xiong, G. Xiao, and R.B. Laibowitz, Phys. Rev. Lett. **71**, 1907 (1993).

[11] P.H.C. Magnee, N. van der Post, P.H.M. Kooistra, B.J. van Wees, and T.M. Klapwijk, Phys. Rev. B **50**, 4594 (1994).

[12] J. Kutchinsky, R. Taboryski, T. Clausen, C.B. Sorensen, A. Kristensen, P.E. Lindelof, J. Bindslev Hansen, C. Schelde Jacobsen, and J.L. Skov, Phys. Rev. Lett. **78**, 931 (1997).

[13] W. Poirier, D. Mailly, and M. Sanquer, Phys. Rev. Lett. **79**, 2105 (1997).

[14] G.E. Blonder, M. Tinkham, and T.M. Klapwijk, Phys. Rev. B **25**, 4515 (1985).

[15] A.V. Zaitsev, Sov. Phys. JETP **59**, 1163 (1984).

[16] C.W.J. Beenakker, Rev. Mod. Phys. **69**, 731 (1997).

[17] C.J. Lambert, J. Phys.: Condens. Matter **3**, 6579 (1991).

[18] Y. Takane and H. Ebisawa, J. Phys. Soc. Jpn. **61**, 2858 (1992).

[19] C.W.J. Beenakker, Phys. Rev. B **46**, 12 841 (1992).

[20] C.W.J. Beenakker, B. Rejaei, and J.A. Melsen, Phys. Rev. Lett. **72**, 2470 (1994).

[21] G.B. Lesovik, A.L. Fauchere, and G. Blatter, Phys. Rev. B **55**, 3146 (1997).

[22] A.I. Larkin and Yu.V. Ovchinnikov, Sov. Phys. JETP **41**, 960 (1975).

[23] A.F. Volkov, A.V. Zaitsev, and T.M. Klapwijk, Physica C **210**, 21 (1993).

[24] K.D. Usadel, Phys. Rev. Lett. **25**, 507 (1970).

[25] M.Yu. Kupriyanov and V.F. Lukichev, Zh. Exp. Teor. Fiz. **94**, 139 (1988) [Sov. Phys. JETP **67**, 1163 (1988)].

[26] C.J. Lambert, R. Raimondi, V. Sweeney, and A.F. Volkov, Phys. Rev. B **55**, 6015 (1997).

[27] Yu.V. Nazarov, Phys. Rev. Lett. **73**, 1420 (1994).

[28] S. Yip, Phys. Rev. B **52**, 3087 (1995).

[29] Yu.V. Nazarov and T.H. Stoof, Phys. Rev. Lett. **76**, 823 (1996); T.H. Stoof and Yu.V. Nazarov, Phys. Rev. B **53**, 14 496 (1996).

[30] A.F. Volkov, N. Allsopp, and C.J. Lambert, J. Phys.: Condens. Matter **8**, L45 (1996); A.F. Volkov and H. Takayanagi, Phys. Rev. B **56**, 11 184 (1997).

[31] A.A. Golubov, F.K. Wilhelm, and A.D. Zaikin, Phys. Rev. B **55**, 1123 (1997).

[32] A.F. Volkov and H. Takayanagi, Phys. Rev. B **56**, 11 184 (1997).

[33] E.V. Bezuglyi, E.N. Bratus', V.S. Shumeiko, G. Wendin, and H. Takayanagi, Phys. Rev. B **62**, 14 439 (2000).

[34] R. Seviour and A.F. Volkov, Phys. Rev. B **61**, R9273 (2000).

[35] W. Belzig *et al.*, Superlattices Microstruct. **25**, 1251 (1999).

[36] Yu.V. Nazarov, cond-mat/9811155 (unpublished).

[37] A.A. Golubov and M.Yu. Kupriyanov, J. Low Temp. Phys. **70**, 83 (1988); W. Belzig, C. Bruder, and G. Schön, Phys. Rev. B **54**, 9443 (1996); J.A. Melsen, P.W. Brouwer, K.M. Frahm, and C.W.J. Beenakker, Europhys. Lett. **35**, 7 (1996); F. Zhou, P. Charlat, B. Spivak, and B. Pannetier, J. Low Temp. Phys. **110**, 841 (1998).

[38] P. Charlat, *et al.*, Phys. Rev. Lett. **77**, 4950 (1996); V.T. Petrashov, R.Sh. Shaikadarov, P. Delsing, and T. Claeson, Pis'ma Zh. Éksp. Teor. Fiz. **67**, 689 (1988) [JETP Lett. **67**, 513 (1998)]; S.G. Lachenmann, I. Friedrich, A. Förster, D. Uhlisch, and A.A. Golubov, Phys. Rev. B **56**, 14 108 (1997); H. Courtois, Ph. Gandit, B. Pannetier, and D. Mailly, Superlattices Microstruct. **25**, 721 (1999).

[39] L.J. Buchholtz and G. Zwicknagl, Phys. Rev. B **23**, 5788 (1981); C. Bruder, *ibid.* **41**, 4017 (1990); C.R. Hu, Phys. Rev. Lett. **72**, 1526 (1994).

[40] Y. Tanaka and S. Kashiwaya, Phys. Rev. Lett. **74**, 3451 (1995); S. Kashiwaya, Y. Tanaka, M. Koyanagi, and K. Kajimura, Phys. Rev. B **53**, 2667 (1996); Y. Tanuma, Y. Tanaka, and S. Kashiwaya, *ibid.* **64**, 214519 (2001).

[41] S. Kashiwaya and Y. Tanaka, Rep. Prog. Phys. **63**, 1641 (2000) and references therein.

[42] J. Geerk, X.X. Xi, and G. Linker, Z. Phys. B: Condens. Matter **73**, 329 (1988); S. Kashiwaya, Y. Tanaka, M. Koyanagi, H. Takashima, and K. Kajimura, Phys. Rev. B **51**, 1350 (1995); L. Alff, H. Takashima, S. Kashiwaya, N. Terada, H. Ihara, Y. Tanaka, M. Koyanagi, and K. Kajimura, *ibid.* **55**, 14 757 (1997); M. Covington, M. Aprili, E. Paraoanu, L.H. Greene, F. Xu, J. Zhu, and C.A. Mirkin, Phys. Rev. Lett. **79**, 277 (1997); J.Y.T. Wei, N.-C. Yeh, D.F. Garrigus and M. Strasik, *ibid.* **81**, 2542 (1998); I. Iguchi, W. Wang, M. Yamazaki, Y. Tanaka, and S. Kashiwaya, Phys. Rev. B **62**, R6131 (2000); F. Laube, G. Goll, H.v. Löhneysen, M. Fogelström, and F. Lichtenberg, Phys. Rev. Lett. **84**, 1595 (2000); Z.Q. Mao, K.D. Nelson, R. Jin, Y. Liu, and Y. Maeno, *ibid.* **87**, 037003 (2001); Ch. Wälti, H.R. Ott, Z. Fisk, and J.L. Smith, *ibid.* **84**, 5616 (2000); H. Aubin, L.H. Greene, Sha Jian, and D.G. Hinks, *ibid.* **89**, 177001 (2002); Z.Q. Mao, M.M. Rosario, K.D. Nelson, K. Wu, I.G. Deac, P. Schiffer, Y. Liu, T. He, K.A. Regan, and R.J. Cava, Phys. Rev. B **67**, 094502 (2003); A. Sharoni, O. Millo, A. Kohen, Y. Dagan, R. Beck, G. Deutscher, and G. Koren, *ibid.* **65**, 134526 (2002); A. Kohen, G. Leibovitch, and G. Deutscher, Phys. Rev. Lett. **90**, 207005 (2003).

[43] Y. Tanaka, Y.V. Nazarov, and S. Kashiwaya, Phys. Rev. Lett. **90**, 167003 (2003).

[44] H. Kashiwaya, A. Sawa, S. Kashiwaya, H. Yamasaki, M. Koyanagi, I. Kurosawa, Y. Tanaka, and I. Iguchi, Physica C **357-360**, 1610 (2001).

[45] Y. Tanaka, Y. Nazarov, A. Golubov, and S. Kashiwaya (unpublished).

[46] T.M. Klapwijk, G.E. Blonder, and M. Tinkham, Physica B & C **109-110**, 1657 (1982).

[47] M. Octavio, M. Tinkham, G.E. Blonder, and T.M. Klapwijk, Phys. Rev. B **27**, 6739 (1983).

[48] G.B. Arnlod, J. Low Temp. Phys. **68**, 1 (1987); U. Gunsenheimer and A.D. Zaikin, Phys. Rev. B **50**, 6317 (1994).

[49] E.N. Bratus, V.S. Shumeiko, and G. Wendin, Phys. Rev. Lett. **74**, 2110 (1995); D. Averin and A. Bardas, *ibid.* **75**, 1831 (1995);

J.C. Cuevas, A. Martin-Rodero, and A.L. Yeyati, Phys. Rev. B **54**, 7366 (1996).

[50] A. Bardas and D.V. Averin, Phys. Rev. B **56**, 8518 (1997); A.V. Zaitsev and D.V. Averin, Phys. Rev. Lett. **80**, 3602 (1998).

[51] A.V. Zaitsev, Physica C **185-189**, 2539 (1991).

[52] E.V. Bezuglyi, E.N. Bratus', V.S. Shumeiko, and G. Wendin, Phys. Rev. Lett. **83**, 2050 (1999).

[53] A. Brinkman and A.A. Golubov, Phys. Rev. B **61**, 11 297 (2000).

[54] Y. Tanaka and S. Kashiwaya, Phys. Rev. B **53**, 11957 (1996); *ibid.* **56**, 892 (1997); Y.S. Barash, H. Burkhardt, and D. Rainer, Phys. Rev. Lett. **77**, 4070 (1996); E. Ilichev, M. Grajcar, R. Hlubina, R.P.J. IJsselsteijn, H.E. Hoenig, H.-G. Meyer, A. Golubov, M.H.S. Amin, A.M. Zagoskin, A.N. Omelyanchouk, and M.Yu. Kuprianov, *ibid.* **86**, 5369 (2001).